

PhO₂: Smartphone based Blood Oxygen Level Measurement Systems using Near-IR and RED Wave-guided Light

Nam Bui

University of Colorado Boulder
nam.bui@colorado.edu

Anh Nguyen

University of Colorado Boulder
anh.tl.nguyen@colorado.edu

Phuc Nguyen

University of Colorado Boulder
vp.nguyen@colorado.edu

Hoang Truong

University of Colorado Boulder
hoang.truong@colorado.edu

Ashwin Ashok

Georgia State University
aashok@gsu.edu

Thang Dinh

Virginia Commonwealth University
tndinh@vcu.edu

Robin Deterding

Children's Hospital Colorado
robin.deterding@childrenscolorado.org

Tam Vu

University of Colorado Boulder
tam.vu@colorado.edu

ABSTRACT

Accurately measuring and monitoring patient's blood oxygen level plays a critical role in today's clinical diagnosis and healthcare practices. Existing techniques however either require a dedicated hardware or produce inaccurate measurements. To fill in this gap, we propose a phone-based oxygen level estimation system, called PhO₂, using camera and flashlight functions that are readily available on today's off-the-shelf smart phones. Since phone's camera and flashlight are not made for this purpose, utilizing them for oxygen level estimation poses many challenges. We introduce a cost-effective add-on together with a set of algorithms for spatial and spectral optical signal modulation to amplify the optical signal of interest while minimizing noise. A light-based pressure detection algorithm and feedback mechanism are also proposed to mitigate the negative impacts of user's behavior during the measurement. We also derive a non-linear referencing model that allows PhO₂ to estimate the oxygen level from color intensity ratios produced by smartphone's camera.

An evaluation using a custom-built optical element on COTS smartphone with 6 subjects shows that PhO₂ can estimate the oxygen saturation within 3.5% error rate comparing to FDA-approved gold standard pulse oximetry. A user study to gauge the reception of PhO₂ shows that users are comfortable self-operating the device, and willing to carry the device when going out.

ACM Reference format:

Nam Bui, Anh Nguyen, Phuc Nguyen, Hoang Truong, Ashwin Ashok, Thang Dinh, Robin Deterding, and Tam Vu. 2017. PhO₂: Smartphone based Blood Oxygen Level Measurement Systems using Near-IR and RED Wave-guided Light. In *Proceedings of SenSys '17, Delft, Netherlands, November 6–8, 2017*, 14 pages.
DOI: 10.1145/3131672.3131696

Permission to make digital or hard copies of all or part of this work for personal or classroom use is granted without fee provided that copies are not made or distributed for profit or commercial advantage and that copies bear this notice and the full citation on the first page. Copyrights for components of this work owned by others than ACM must be honored. Abstracting with credit is permitted. To copy otherwise, or republish, to post on servers or to redistribute to lists, requires prior specific permission and/or a fee. Request permissions from permissions@acm.org.

SenSys '17, Delft, Netherlands

© 2017 ACM. 978-1-4503-5459-2/17/11...\$15.00
DOI: 10.1145/3131672.3131696

1 INTRODUCTION

Blood oxygen level, which is often indicated through oxygen saturation measurement (SpO₂), has long been recognized as an important indicator of patient's wellbeing and extensively used for clinical diagnosis [8, 25, 26, 37, 38, 58], owing to the critical role of oxygen in the operational functions of vital organs and tissues. If the human body cannot exchange and deliver oxygen efficiently, the amount of oxygen available for organs throughout the body becomes insufficient, which can lead to long-term damage of individual cells, heart, brain, etc. or short-term malfunctioning of other vital organisms [11, 35, 36]. Therefore, accurately measuring SpO₂ with high frequency is critical to not only monitor the key organ's wellbeing but also provide early warning signs of abnormalities and potential health problems. There have been extensive literature and commercial solutions both invasive and non-invasive to measure SpO₂. Pulse oximetry is a common measurement of SpO₂ for in-hospital and in-home environments. A typical noninvasive pulse oximetry system requires a dedicated pulse oximetry hardware and software [3, 6, 7, 14, 15, 17, 18, 20–22, 41, 43, 47, 54, 60, 61]. The device projects light beams at specific wavelengths deep into its users' finger, toe, earlobe, or other location. Lights hit dedicated photo electrodes after penetrating through multiple layers of skin, artery, and blood cells. The electrodes are designed to receive only those within a desired wavelength range. The intensity of the received light carries the information that can be used to estimate the SpO₂ level of the blood cells that the lights have gone through [34]. While the current SpO₂ measurement largely relies on these dedicated pieces of equipment owing to its high accuracy and reliability, they have several undesirable features, especially for frequent measurement. First of all, a user needs to acquire the device by purchasing it (directly or indirectly through insurance or doctor prescription). Second, these pulse oximetry devices require users to carry with them for performing frequent measurement while they are in very day life (as opposed to be in hospital). This requirement often reduces the usability of the device since patients have tendency to forget their devices, fail to charge, or misplacing them [59]. Moreover, with the current form factors (e.g. finger clip-on, earlobe clip-on, or finger wrap around), these devices does

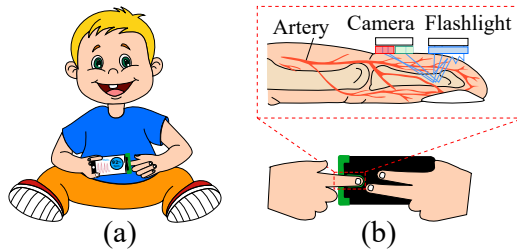


Figure 1: PhO₂ and its general view for SpO₂ measurement. (a) A person is placing his index finger on PhO₂ add-on to check his SpO₂ level. (b) A back view of PhO₂ use in which the add-on covers the phone's flashlight and back camera and a zoomed-in visualization of how PhO₂ works.

not always fit well on patients with different finger and earlobe sizes. For example, a 5 year old boy would have a very different finger size with an adult and also have a different finger size when he turns 6. The ill-fitting of the device leads to significant estimation errors [13].

With the advent of smart phones, most of which are equipped with flash lights and camera, many systems have been proposed using these functions to capture various blood properties. However, none of the existing technologies and systems has the ability to accurately estimate SpO₂ by using built-in sensors in smartphones. For example, using external light sources such as an incandescent light bulb or a group of LEDs, HemaApp [61] from the University of Washington takes advantage of a clever machine learning technique to measure the hemoglobin concentration using the phone's camera. These additional light sources, however, are not pervasive and have restricted usage in modern smartphones, in which an IR filter is employed as part of the camera lens [24]. In addition, HemaApp attempts to estimate the hemoglobin count as opposed to estimating SpO₂. Existing works on estimating SpO₂ using the built-in flashlight and the camera of off-the-shelf smartphones include the systems proposed by Hodgkins et. al. [17] and iCareOxygenMonitor [20]. However, all of them provide a very low accuracy and not intended for clinical use. More details about their performance is presented in the evaluation section (Section 8). The low accuracy is the result of the fundamental challenges when one tries to repurpose the camera and flashlight for SpO₂ measurement.

Challenges: First, most of smartphone flashlights do not include the IR wavelength, which is a critical component for non-invasive SpO₂ measurement. Second, while most of state-of-the-art smartphone-based techniques are using a linear regression model to convert from pulsatile ratio to SpO₂ level, such conversion does not work properly in practice due to the impact of users' finger movements, pressure, contacting area, pulse amplitude, and ambiguity of converting from light intensity to RGB measurement of the camera. Third, the smartphone's camera picks up most of the lights from the flashlight including both hemoglobin responsive and hemoglobin non-responsive wavelengths. While the pulsatile is buried under a small intensity change of the hemoglobin responsive light, this pick up mechanism makes the collected light intensity of the camera non-usable for SpO₂ measurement. Forth, user's finger movement and finger pressure against the camera during measurement significantly affect the estimation quality. SpO₂ measurement

relies on sensing user's pulsatile waveform whose amplitude is shorter than that of other human-generated movements. A tiny shift of our finger possibly magnifies the amplitude or even shatters the signal which consequently has a significant impact on the prediction. Pressure control is as crucial as finger stabilization because strong pressure halts the blood flow in the arteries inside our finger tips. As a result, pulsatile pattern disappears, leading to the measurement inaccuracy. Observation from commercialized pulse oximeters showed that they halt their prediction if the input signal is distorted. Conventional wisdom has not yet to distinguish between motion of finger and inadequate pressure. In most of the existing systems, users only receive a warning saying that their finger is out of the region which makes it difficult for users to adjust the pose of their finger or modify how hard they should press on the camera.

In this paper, we propose a novel mobile oxygen saturation measurement system, named PhO₂, that has a potential to accurately provide the SpO₂ level in real time using smartphones' camera and flashlight. Specifically, as demonstrated in Figure 1, PhO₂ is a phone-based system that includes a hardware add-on designed with optical filters of different wavelengths and snapped on the phone as simply as using a phone case. By leveraging the advancement of 3D printing technology and off-the-shelf filters, our add-on is lightweight and does not affect normal functionality of the phone's flashlight or camera. Moreover, PhO₂ produces two light beams at separate wavelengths from single light source with the use of the add-on. The add-on also helps stabilize users' finger during the SpO₂ measurement and does not prevent the phone's camera from normal use of taking pictures. However, due to limitations of camera hardware, the reflected light captured by PhO₂ device needs to be further processed using dedicated algorithms to obtain usable PPG signals and reliably estimate the SpO₂ level. In particular, PhO₂ real-time model takes streamed frames to evaluate the appearance of possible artifacts and extract the PPG signal of high quality. The high-quality signal is finally input into a regression-based optimization model to calculate the SpO₂ level.

We made the following contributions in realizing the proposed PhO₂, a phone-based SpO₂ level estimation system:

- We develop a lightweight, cost-effective, and portable smartphone's add-on allowing mobile device to measure SpO₂ level accurately and reliably.
- We propose an optical spatial separation technique to extract near infrared (NIR) and red lights from the camera's flashlight. As the NIR and red lights are hemoglobin responsive, their intensity variations are analyzed to infer SpO₂ ratio.
- We devise algorithms to identify the human motion artifact and pressure estimation that provide the best performance of PPG estimation and therefore improve the accuracy of SpO₂ measurement.
- We design a non-linear calibration technique to infer the SpO₂ level from the observed intensity from two separated lights mentioned earlier.
- We verify the performance of our proposed solution with the gold standard noninvasive SpO₂ measurement device. The PhO₂ obtains 3.5 % of accuracy with 80% of confidence compared to the gold standard device.

- We confirm that the PhO₂ device receives very positive feedback from 10 trial users.
- We discuss potential applications of our proposed technique. In particular, we envision that the spatial optical dividing techniques can be used to extract the desired wavelengths for any light-based applications.

2 RELATED WORK

In this section, we present a thorough survey of existing literature on SpO₂ estimation to compare and contrast with our proposed system, PhO₂.

Pure phone-based solutions. Multiple systems for easy-to-access oxygen level measurement have been developed in the form of a mobile app. Existing apps such as Instant Pulse Oximeter [21], Vigor SpO₂ [60], Instant Pulse Rate [22], Heart Rate Pulse Oximeter [15], and iCare Oxygen Monitor [20]) follow the same schema in which a single streaming video clip with duration from around 10 to 15 seconds is processed to extract the heartbeat and oxygen level. The key shortcoming of these systems is their inaccuracy due to the challenges that we have mentioned in the previous section. PhO₂, in contrast, identifies and addresses these challenges to significantly improve its performance.

Hardware-aided phone-based alternatives. The most relevant technique to our work is HemaApp [61], which uses mobile phone camera with the aid of high power incandescent light bulb or a group of LEDs attached in front of camera lens, to measure the hemoglobin concentration, but not the SpO₂ level. Although the system was cleverly designed and reportedly works well to estimate hemoglobin concentration, it strictly depends on the availability of external IR light source and relies on the ability to capture IR light of phone’s camera, which is not available in off-the-shelf devices with IR filter (we empirically prove this with the evidence of spectrum analysis of lights collected from iPhone 4, Galaxy S4, S5, and Note 3 in the next section). Our system, in contrast, is not only free of hard-to-access additional equipment, but also independent of external IR source, which makes our app compatible with most of off-the-shelf smart phones.

Dedicated pulse oximeters. Pulse oximeters have been developed and widely used since 1930s. The designs and products have evolved from devices which are large, heavy, expensive, and available only for military and sleep laboratories [16] to ones that are cheap, small (ear-lobe usage [3, 14, 41, 43], finger tip compatible), and pervasive (e.g. FDA-approved devices can be bought easily from \$30 [6, 7, 18, 47, 54]). There are also existing variations of pulse oximeter such as forehead-type [2, 4, 9, 50, 63], tracheal-type [5], and ring-type [19]. At the moment, the quality and performance of cheap pulse oximeter still raise concerns for the healthcare community [31]. Other dedicated hardware that can be connected to smart phones includes Phone Oximetry [44] and audio-based pulse oximetry [45]. They use the commercial pulse oximetry probe in connection with software on smart phone to calculate the SpO₂ level. However, these solutions require dedicated hardware to be purchased, users carry the hardware with them for frequent monitoring and sometimes does not fit with patient’s finger or earlobe, which reduces its accuracy. In comparison, PhO₂ frees users from carrying additional device and using their mobile phone instead while maintaining the high level of accuracy.

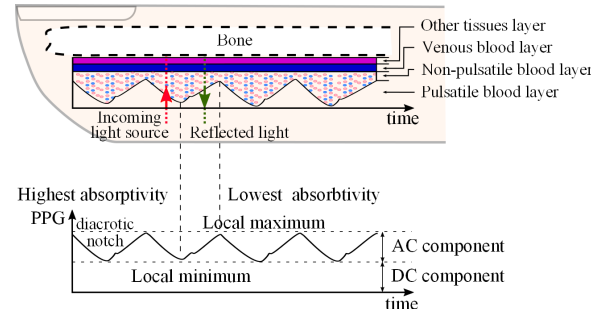


Figure 2: Non-invasive SpO₂ measurement illustration in which an incoming light source penetrates different layers of a finger then reflects back to produce a PPG signal that is captured by a dedicated photoreceivers

Finger pressure detection and user guidance studies. Research on phone-based SpO₂ measurement [29, 52] or oxygen concentration (HemaApp) [61] left the problem of finger posture and unappropriate pressure remains untouched. However, in clinical literature, Hayes et. al. [12] points out that finger pressure is one of the main cause of error in pulse oximeters. Therefore, with PhO₂, the pressure at contact area is carefully considered. A set of algorithms are proposed to estimate the improper pressure events from which a feedback is launched to notify users and suggest pressure adjustment to users. To the best of our knowledge, pressure control has not been explored to improve signal acquisition for SpO₂ measurement for neither phone-based nor dedicated-hardware solutions. The techniques derived here, therefore, can benefit the current design of commercial dedicated pulse oximeters as well.

3 PRINCIPLE OF SPO₂ MEASUREMENT

In this section, we present in details the background of noninvasive oxygen saturation (SpO₂) measurement from its first principles, through derivation, to the practical techniques. This section sets the foundational understanding of the existing SpO₂ estimation techniques, from which PhO₂ is built up on.

Oxygen saturation (SpO₂) is the percentage of oxygen in arterial blood measured by taking a ratio of the hemoglobin with oxygen to the sum of oxide hemoglobin and dioxiide hemoglobin. Therefore, SpO₂ level can be obtained by $SpO_2 = \frac{\rho_{O_2}}{\rho_{O_2} + \rho_{Hb}}$ in which ρ_{O_2} and ρ_{Hb} are the concentration of hemoglobin with and without oxygen, respectively. In an invasive SpO₂ estimation approach, ρ_{O_2} and ρ_{Hb} can be calculated through a blood gas test in which blood samples are collected and count the number of hemoglobin binding oxygen [23]. Though this technique is accurate, it is invasive and costly. Therefore, non-invasive alternatives have been proposed and are much more widely used.

Non-invasive SpO₂ measurement. The key idea is to evaluate the attenuation of light penetrating through multiple layers inside human finger and mark down the “pulsatile” waveform on a photon detector. This method is called photoplethysmography (PPG), which was originally developed as an alternative to measure cardiovascular pulse waves.

1. *How is pulsatile wave captured?* Human finger includes multiple layers such as skin, pulsatile blood layer, venous blood layer, other tissues layer, and the bone (as illustrated in Figure 2 (top)). When a light beams into the finger, the reflected component, which

can be captured by photodiode, has different intensity as shown in Figure 2 (bottom). The fluctuating patterns in the light intensity are caused by the following characteristics: (1) the local minimum value of the light's intensity, called *DC component*, represents the intensity of light that is reflected from the static component inside human fingers, such as bone, venous blood layer, and non-pulsatile blood layer; and (2) the maximum variance of the reflected light intensity, called *AC component*, is defined by the variance of the pulsatile blood layer. Using the later characteristic, the variance of the reflected signal intensity directly correlates to the pulsatile waveform generated by cardiovascular waves [34].

Let's consider the beaming light that has the intensity of I_0 and the intensity of the reflected beam is I , the decrease of the intensity can be obtained from Beer-Lambert's law [32] using the following equation: $I = I_0 e^{-\varepsilon(\lambda)\rho d}$. In that, $\varepsilon(\lambda)$ is the absorptivity – a function of wavelength – and c and d are the concentration and depth of the medium, respectively. When light traverses through multiple media, the total absorption is the summation of all the media coefficients in the exponential term $I = I_0 e^{-\sum_i \varepsilon_i(\lambda)\rho_i d_i}$.

Considering oxyhemoglobin, deoxyhemoglobin, and tissues as the three main media inside the finger that let light traverse through, the light intensity after reflected can be represented as:

$$I = I_0 e^{2(-\varepsilon_t(\lambda)\rho_t d_t - \varepsilon_{Hb}(\lambda)\rho_{Hb} d_a - \varepsilon_{O_2}(\lambda)\rho_{O_2} d_a)} \quad (1)$$

In that, ε_t , ε_{Hb} , and ε_{O_2} represent the extinct coefficients of other tissues, pulsatile, and non-pulsatile blood layers, respectively. d_t and d_a denote the thickness of tissue and blood medium, respectively. The key factors are the concentration denoted as ρ_t , ρ_{Hb} , and ρ_{O_2} respected to each medium. The optical path length of tissue layer d_t might be stable while arterial part d_a varies periodically following cardiac activities. Therefore, the light intensity received when the blood level is at minimum (in diastolic phase (d_a^s)) and at maximum (in systolic phase (d_a^e)), denoted as I_p and I_b , can be presented as:

$$I_p = I_0 e^{2(-\varepsilon_t(\lambda)\rho_t d_t - \varepsilon_{Hb}(\lambda)\rho_{Hb} d_a^s - \varepsilon_{O_2}(\lambda)\rho_{O_2} d_a^s)} \quad (2)$$

$$I_b = I_0 e^{2(-\varepsilon_t(\lambda)\rho_t d_t - \varepsilon_{Hb}(\lambda)\rho_{Hb} d_a^e - \varepsilon_{O_2}(\lambda)\rho_{O_2} d_a^e)} \quad (3)$$

Taking the ratio of I_p and I_b , we obtain the form in which some of the variables are called.

$$\frac{I_p}{I_b} = e^{-2(\varepsilon_{Hb}(\lambda)\rho_{Hb}(d_a^s - d_a^e) + \varepsilon_{O_2}(\lambda)\rho_{O_2}(d_a^s - d_a^e))} \quad (4)$$

The absorptivity change can be obtained by taking the natural logarithm of the above equation and scale by half $A = 0.5 \ln(\frac{I_p}{I_b}) = \varepsilon_{Hb}(\lambda)\rho_{Hb}\Delta d_a + \varepsilon_{O_2}(\lambda)\rho_{O_2}\Delta d_a$, where $\Delta d_a = d_a^s - d_a^e$ is another unknown variable. To remove this value, we apply the formula for one particular wavelength. In the commercialized pulse oximeter, the wavelengths corresponding to Red and IR are selected to calculate the absorptivity ratio (Figure 3) [28, 51, 68]. We can rewrite the following equation to take redundancy factors into consideration.

$$A = \varepsilon_{Hb}(\lambda)\rho_{Hb}\Delta d_a + \varepsilon_{O_2}(\lambda)\rho_{O_2}\Delta d_a + A_\eta \quad (5)$$

Finally, we derive the form of the differentiation absorptivity as follow.

$$\frac{dA}{dt} = \varepsilon_{Hb}(\lambda)\rho_{Hb} \frac{\Delta d_a}{dt} + \varepsilon_{O_2}(\lambda)\rho_{O_2} \frac{\Delta d_a}{dt} \quad (6)$$

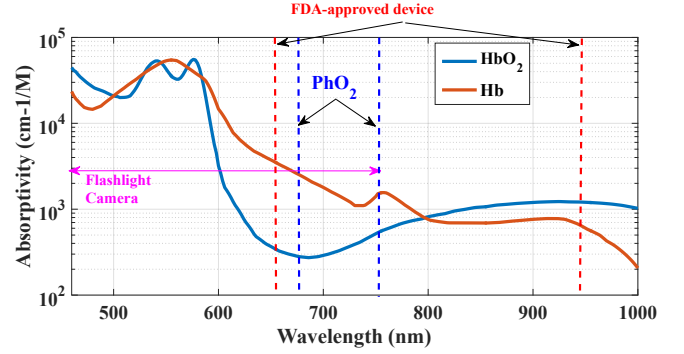


Figure 3: Absorptivity of hemoglobin and dehemoglobin versus wavelengths.

$$R = \frac{d(\ln(\frac{I_p(r)}{I_b(r)}))/dt}{d(\ln(\frac{I_p(ir)}{I_b(ir)}))/dt} \approx \frac{I_p(r) - I_b(r)}{I_b(r)} = \frac{AC(r)}{DC(r)} \quad (7)$$

$$= \frac{\varepsilon_{Hb}(r)\rho_{Hb} + \varepsilon_{O_2}(r)\rho_{O_2}}{\varepsilon_{Hb}(ir)\rho_{Hb} + \varepsilon_{O_2}(ir)\rho_{O_2}}$$

Recall that the measurement of SpO_2 is calculated by $SpO_2 = \frac{\rho_{O_2}}{\rho_{O_2} + \rho_{Hb}}$. By substituting ρ_{O_2} and ρ_{Hb} into Equation 7, we first isolate the term:

$$\rho_{O_2} = SpO_2(\rho_{O_2} + \rho_{Hb}); \rho_{Hb} = (1 - SpO_2)(\rho_{O_2} + \rho_{Hb}) \quad (8)$$

Hence, Equation 7 after the replacement becomes:

$$R = \frac{\varepsilon_{Hb}(r)(1 - SpO_2) + \varepsilon_{O_2}(r)SpO_2}{\varepsilon_{Hb}(ir)(1 - SpO_2) + \varepsilon_{O_2}(ir)SpO_2} \quad (9)$$

By exchanging the position of absorptivity r and SpO_2 , SpO_2 can be derived from the following final formula:

$$SpO_2 = \frac{\varepsilon_{Hb}(r) - \varepsilon_{Hb}(r)R}{\varepsilon_{Hb}(ir) - \varepsilon_{Hb}(r)R + [\varepsilon_{Hb}(ir) - \varepsilon_{Hb}(r)]R} \quad (10)$$

2. *Why do we need two wavelengths?* The typical hardware of the pulse oximeter includes two light sources (Red and IR wavelengths) at the transmitter side. On the receiver side, two photon detectors are used to measure the intensity of the two lights after going through our finger (transparent type) or reflecting at contact point (reflectance type). When using flashlight and camera as transceivers, the transmitter and receiver are placed on the same side. In human blood, the major of hemoglobin components (called functional hemoglobin) are oxygenated hemoglobin (oxyHb) and deoxygenated hemoglobin (around 98%), other 2% (called dysfunctional hemoglobin) include MetHb and CoHb. Those two components absorb unequal amount of light at different wavelengths. In order to measure the oxygen saturation level, two wavelengths must be used to compare how much each light is absorbed by blood. Depending on the amount of oxyHb and deoxygenated Hb present, the ratio of amount of the 1st light absorbed compared to the amount of the 2nd light absorbed will be obtained and inferred the SpO_2 level.

3. *Which wavelengths are used?* In traditional pulse oximeter design, RED light (660nm) and near-infrared (IR) light (940nm) are used to maximize the differences between absorption level of oxygenated and deoxygenated hemoglobin. However, IR lights are not producible by smart phone's flashlight and its camera cannot

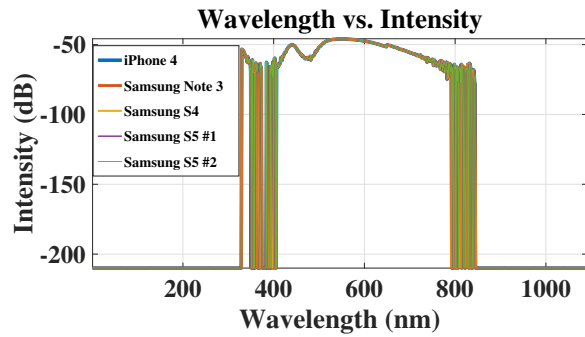


Figure 4: The intensity of different wavelength generated by flashlight from different smartphones.

capture the light at IR frequencies. Indeed, our spectrum analysis results for flashlight of various phones (iPhone 4, Galaxy S4, S5, and Note 3) show that there is no IR components in the flashlight (Figure 4). Furthermore, most of latest camera lens come with built-in IR filter for improving normal picture quality, which makes it impossible to record IR light in off-the-shelf phone. Due to those difficulties, our system must be able to select the 2 lights with the most appropriate wavelengths that works with smart phones while giving the recognizable absorption ratio between oxygenated and deoxygenated hemoglobin.

All in all, to measure SpO₂ level accurately from off-the-shelf smartphones, the system needs: (1) two different hemoglobin-responsive light sources; (2) These two lights must be spatially separated so that the receiver can distinguish their impact on the camera sensor; (3) The camera has to be able to infer from the intensity to the pulsatile variance for SpO₂ measurement; (4) The obtained pulsatile must be usable for properly inferring SpO₂ measurement regardless of changing subjects or smartphones.

4 SYSTEM OVERVIEW

In this section, we first present the challenges in realizing PhO₂ then discuss different components of the system that are designed to address these challenges.

4.1 Design challenges

1. *Smartphone's flashlight cannot generate IR lights.* In literature, Red and IR light are the two wavelengths that yield the highest accuracy and are used in most FDA-approved noninvasive pulse oximeters (See Section 3). However, since camera flashlight is made to generate lights that are capturable by camera, the light that it produces is manufactured so that it falls only within the visible range. To confirm this phenomenal, we conducted an experiment to analyze the wavelength of lights from modern smartphones (including Galaxy Note 3, S5, S4, and iPhone 4). We used Ando Model AQ6315E Optical Spectrum Analyzer [42] for this experiment. The result in Figure 4 shows that the flashlight contains only the light within the visible and near IR ranges (wavelength from 400nm to 779nm). To overcome this problem, instead of selecting the Red and IR lights as in the ideal cases, we make use of the Red wavelength (670 to 690nm) and near IR (NIR) wavelength (700nm to 779nm) from the flashlight (see Section 5). This modification requires a new model for us to identify the wavelengths that work best. We present our wavelength selection technique in Section 5. 2. *NIR filter needs*

to be thin. To construct our add-on, the filter must be thin enough to avoid signal lost due to optical absorption and scatter. However, there is no NIR filter on the market that fits our need due to its minimum thickness. The minimum thickness that we found for NIR filter is usually around 5.1 mm [40]. We propose to take advantage of the non-linearity of the basic color filter (green color) to address this problem, as can be seen later in Section 5. As a result, our designed filter has the thickness of less than 1.5mm, which is suitable for most mobile add-on form and minimizes the distance between the human finger, the light source, and the camera.

3. *Smartphone camera is noisy.* The smartphone camera is designed to pick the light component that has high intensity within the visible range. It usually gathers the whole range of transmitted white light from the flash. Hence, the light intensity variance captured by the camera after going through user's finger is very noisy due to the impact of non-responsive hemoglobin wavelengths. A light divider and a set of separation algorithms are required to create two separated light sources for SpO₂ measurement (See Section 5- 6).

4. *Human finger pressure has significant impact to the accuracy measurement.* The ratio between the two light sources helps to remove the impact of non-AC component. However, given the sensitive of the camera sensor, the pressure of placing the human finger as well as the size of the contacting point place an important role to the accuracy of estimation. The finger movement and pressure have a large impact to the accuracy of measurement. Therefore, online feedback system is needed to make sure that the finger movement does not happen during the experiment and the user provides sufficient pressure to the device (See Section 6.1).

5. *Legacy linear regression model for light intensity to SpO₂ is not applicable.* Linear regression model is applied for most of pulse oximeter devices as the light beams (photo diodes) and photodetectors are specifically designed for SpO₂ measurement [57]. When using the flashlight and camera from the phone, linear regression model cannot be used due to the impact of flashlight's noises (non-responsive hemoglobin wavelengths) and the light intensity to RGB conversion, the human pressure, contacting area, and finger movements to camera' readings. Therefore, the SpO₂ calculation model must take all these effects into account (we proposed a new mapping model for camera-based method in Section 7).

4.2 Proposed System

In this section, we outline the structure of our system in measuring oxygen level by adapting only parts and functions built in off-the-shelf smartphone as illustrated in Figure 5. The specific design of add-on helps to isolate lights with two different wavelengths. The raw data is recorded and put into small chunk which undergoes multiple steps of processing to give out the final prediction. On top of that is a mechanism that helps to ensure that the quality of signal is not effected by motion artifacts and inappropriate pressure.

Optical spatial divider for wavelength separation. Different from the incandescent lamp, lights coming from flash in smartphone does not contain components whose wavelength is larger than 780 nm. Current pulse oximeter relies on the lights that reach to the IR frequency which is unobtainable flashlight is the only source of illumination. We can borrow that outer sources from external components such as LED or incandescent lamp which was

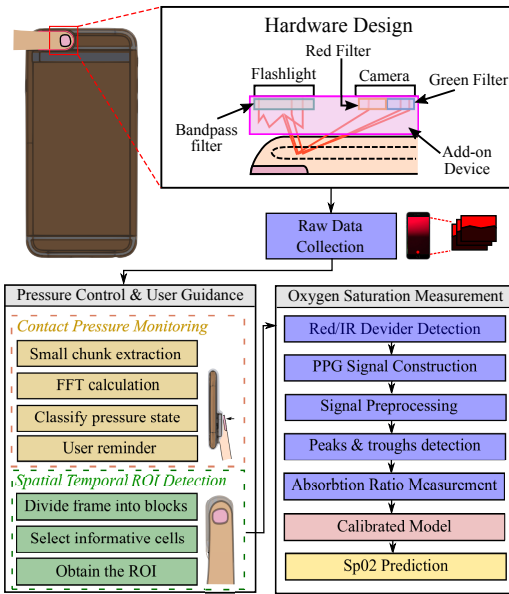


Figure 5: Overall system design and architecture of PhO₂.

introduced in HemaApp [61]. Then power is an issue. In order to use only the flashlight source, it is essential to select a substitute wavelength for IR in the range that is given by smartphone flashlight. The lights with wavelengths less than 600 nm will be absorbed by the red skin pigmentation. Therefore, our interest range is from 600nm to 779nm and the one that maximize the angle of relational curve between Red and IR (figure) is our candidate. The arrangement of one optical polyester filter and a narrow band borosilicate glass filter, following the two frequencies, on camera surface is our system's unique signature in dealing with wavelength separation and without the need of additional illumination sources. The structure is integrated within the add-on, including a special feature for the finger-stabilization, which attaches firmly to any smartphone fit to the design.

Finger pressure control. While existing systems allow signals with motion interference to be pruned into their main functions, we argue that PPG signals are overwhelmed by other movements and thus cannot be completely separated. The design of PhO₂ will not take them into account, in fact, they need to be eliminated or utilized to inform users in advance of the struggle. The system can (1) differentiate between motion and the fluctuation from pulsatile nature within a small number of frames, (2) sense the pressure level by only vision features and (3) notify users whether the signals happen to be noisy by a caution attached with a clear instruction. The real-time function provides a more generic picture to interpret the respiratory conditions rather than getting the result after specified minimum wait.

The prototype is supported by a set of multi-stage processes from manipulating with the raw data, smoothing, processing the outcome signal to the key features of the estimation of absorption ratio and its reference to the oxygen level. Each of the procedures critically contributes to the success of our prediction model. Here, we address every single piece of the system started from the point that has been assumed for a long time to be trivial.

Optimal relational model. Given the frequencies in that range without the IR, the variation of ratio R is small compared to the change of SpO₂ making the linear calibration becomes inaccurate. Since, the pulse oximeter adapt Red and IR lights, the relation between absorption ratio and R (Eq. 7) can be approximated by a linear equation. We argue that using the original equation with a larger number of variables to map between R and measured SpO₂. In this paper, we propose a solution to formulate the problem using descent gradient, to be more specific, the Levenberg-Marquardt [] method helps to identify the best fitting curve for our model. The high saturation of flash light versus the dense and focus beam of LED diode returns a large number of outliers which defects the estimation. Our expectation is to select only the pairs, R and SpO₂, which contributes most to the regression curve. Random Sample Consensus (RANSAC) is developed to divide the inliers and outliers of data points without any prior knowledge about the model. Using iterative cross-validation, RANSAC filters the outliers at each iteration and reserves only the meaningful data points. The hybrid structure of Lavenberg-Marquardt and RANSAC gives a strong fitting curve which eliminates the outliers in the data and solve the high complexity problem such as the relation between SpO₂ which is a fractional equation with four degrees of freedom.

5 OPTICAL SPATIAL DIVIDER

In this section, we will introduce the design of add-on and discuss how the filters satisfy the non-invasive measuring prerequisites. From the Beer-Lambert law, the problem of light scattering is negligible, which does not reflect the real situation correctly. Moreover, the diffusion of flashlight and other sources from the environment can reduce the system performance. To minimize the distortion, we design a special add-on to (1) prevent the interference of unwanted components from the natural source, (2) navigate the light toward camera region, (3) stabilize a finger during the recording session, and (4) play a role as a shield to protect the lens behind. Using SolidWorks [56] software for design and a 3D phone model, we create the add-on with specific features that can conveniently snap on top of the corresponding device and easily be removed for normal usage. Right above the camera region is the finger-stabilizer having a curve of finger tip. The feature allows users to easily slide their finger in, also, leaves more space for lights to bounce off the finger and hit the camera lenses. The component also prevents user from pressing too hard that halts blood to flow into their vessels, thus resulting in the failure to capture pulsatile wave. The material is chosen to be stiffest and manufactured with a very fine-grained resolution.

The two lenses are positioned to equally divide the image into two regions for Red and NIR respectively as illustrated in Figure 6. Following the Plank equation, NIR light has smaller energy than the visible one and thus needs long exposure time to leave a trace on camera sensor. The CCD function uses a pool of electrons to measure the intensity. Obviously, the visible light with its strong energy will have a better chance to fulfill that pool rather than the NIR. We placed a band-pass optical filter covering the flashlight to reduce the portion of visible components and allow for more NIR to come in and collide with the CCD sensor.

While most of color-filter is capable to block all the unwanted colors, the near IR component will always go through the color

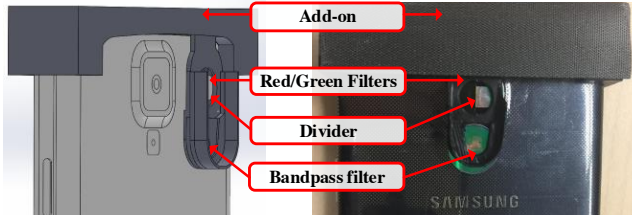


Figure 6: PhO₂ hardware design (3D model - left, Prototype - right)

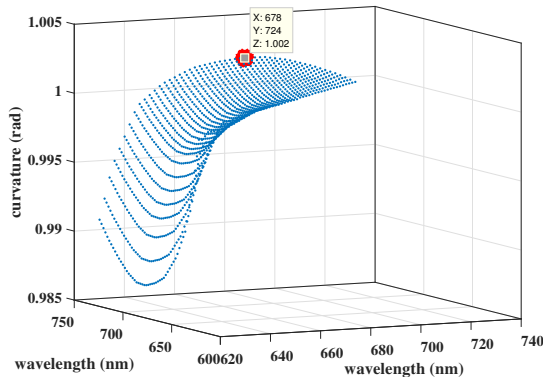


Figure 7: The curvature level of different wavelength combination.

filtering. We design two filters and attach them to the smartphone's camera. The first filter absorbs the Red light at wavelength 680nm (20nm bandwidth) [1] and a green filter [30] to allow the near IR and green color lights to pass through. The second filter removes the red component and only allows the light component that are highly absorbed by the red skin (wavelength less than 600nm [55]) to pass through. Fortunately, the later filter also allows the NIR light component to go through it. By carefully designing those two filters, we obtained two frequency components in the light (Red after the Red filter and NIR after the green filter.) The precise wavelengths need to be identified for the measurement of oxygen level. The research of Karlen *et.al* [27] about the correlation between SpO₂ and absorptivity ratio (R) with respects to different combinations of light source indicates that the cultivate of the relational curve between SpO₂ and R can help to identify the wavelengths. The large angles has a better performance according to [27]. We replicate that simulation for those lights having wavelength from 600 nm to 750nm and calculate the curvature level of angle between the relational curve and the vertical axis. From Figure 7 the combination of lights at 678nm and 724nm has the highest curvature at 1.002 radian. We select those as the possible candidates and search for all the neighbours to identify the optimal pair.

6 PHOTOPLETHYSMOGRAPHY SIGNAL EXTRACTION

In this section, we present our solution for pressure correction which is based on the fact that different levels of pressure can effect on the pulsatile shape. To further improve the quality by cutting off the uninformative areas within a frame, we introduce an algorithm to extract only blocks having a strong FFT peak that associates with the clear pulse rate.

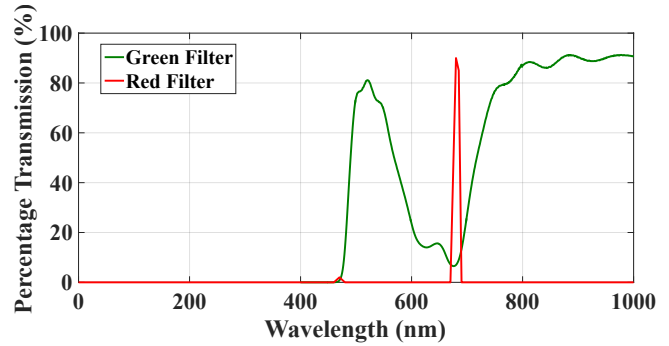


Figure 8: Green/Red filter characteristics. The NIR component is observable through the green filter while Red component is blocked. The Red filter only allows the light with wavelength from 670nm to 690nm go through.

6.1 Mitigating Impacts of User Behaviors

Influences to signal quality. As we stated in previous section, the PhO₂ system uses the non-ideal light source (phone flashlight) and receiver (recorded image frames) which has multiple drawbacks and challenges. These includes the uncontrollable light source (i.e. phone flashlight) and image captured from IR-filter-equipped off-the-shelf phone camera. Those two factors are highly sensitive to light channel interference between the flashlight and camera. Theoretically, our system must record reflected light from patients' finger at extremely close distance in order to extract the PPG signal from the stream of video. Thus, even a slightly interference to the channel between the light source and receiver would cause certain consequence to the signal quality (i.e., reflected light and captured images). We investigate the abnormal changes in our PPG signal in order to search for the causes of interference. Based on recorded data from subjects and their PPG signal analysis, we find out that the unavoidable sources of interference include (1) subject's body movement, (2) miniature movement at the finger tip due to human organ activities, and (3) unawareness of subject's finger pressure on the device.

First of all, human body are subjected to displacement of breathing process. When inhaling or exhaling, the upper body parts (i.e. abdomen, chest and shoulder) fluctuate at respiratory frequency. While measuring SpO₂, the subject is instructed to put their hand and finger to be 'stable' on the device. However, at this so-call 'stable' posture, the deltoid and pectoralis minor muscle group keep moving the arm and hand back and forth slightly. Thus, a small displacement at the contact point fingertip and camera is generated, which lead to the abnormal change in received PPG signal.

Second, each heart beat, which ejects blood into the vessels, causes a repetitive motion in human body. This phenomenon is called heart ballistic forces, which can me measure from ballistocardiography (BCG) signal. These BCG signal can be easily observed by adding sensors to everyday objects or human body. Each blood pump cycle generated pulses that can be observed from all part of human body even the finger tip in our case. Those pulses also create miniature changes at the contact point, which affect the intensity of recorded frames. This leads to the abnormal patterns of the PPG signal.

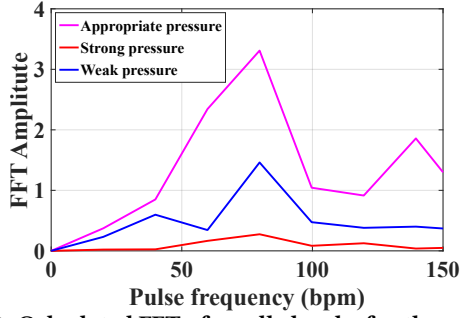


Figure 9: Calculated FFT of small chunks for three pressure states.

Lastly, while using our system, subject is observed to change their pressure of contacting point unconsciously. The digitorum profundus and flexor digitorum superficialis muscle group, which control the movement of fingers and finger tips, tend to move slightly even when the subject is at stable and relaxing position. This causes the most influence to the surface at finger and flashlight/camera, in such case inappropriate pressure causes the intensity of received signal to be overstimulated or too low. Fortunately, by analyzing the recorded frames, our system can successfully detect whenever the subjects' finger is at wrong pressure degree.

Mitigate the pressure problem. Pressure detection has been addressed for usage of mobile phone camera and flash [33]. In addition, motion artifacts and movement detection for traditional PPG data collector and pulse oximeter have been proposed in [27, 64–66]. SpO₂ is designed with pressure detection algorithm to deal with the problem when subjects' finger applies the force on device incorrectly.

Every N seconds chunk of recorded video (i.e. $30N$ frames) is processed and extracted the mean intensity in red channel of each frame. The fluctuation or peak-to-peak variation of this sequence have large differences. With the knowledge that this sequence also represents part of the PPG signal, we calculated its FFT with respected to heart beat frequency (example shown in Figure 9 for more fine-grained resolution and better detection decision. Subjects' press behavior is classified into three categories: (1) strong press, in which intensity sequence is increased, no pulse is observed from recorded video; (2) weak press, in which intensity sequence is reduced, pulse is barely observed; and (3) normal/appropriate press, in which pulse is clearly observed, PPG signal is extracted without abnormalities.

The algorithm can be minimizes up to 1 second window at 0.5 seconds overlap and still detect the wrong subjects' finger posture. By detecting the correct position of bad pressure, our system smooths the extracted PPG signal and gets rid of abnormal error calculation to the final result. Ideally, the system can scan for bad posture at the basis of every 0.5 seconds and notify to the subjects while measuring SpO₂ in real-time so that they can adjust the pressure by themselves.

6.2 ROI and Red-IR Divider Detection

Although the pressure is detected and provides an online feedback to the user, the contacting area between human finger skin and the camera filters are not even. We need to detect the region of interest

Algorithm 1: Borderline detection using K-means clustering.

input : I - input image with the divider.
output : $ListId_k$ List index of pixels in each region.

- 1 Initialize values for the means of each region μ_1 and μ_2 respectively.
- 2 /* Finding optimal means and their corresponding list of pixels.*/
- 3 **for** $t = 1 \rightarrow MaxNumberOfIteration$ **do**
- 4 $ListId_k \leftarrow []$;
- 5 **for** $i = 1 \rightarrow NumberOfPixel$ **do**
- 6 $\hat{k} = \operatorname{argmin}_{k=1,2} d(p(i), \mu_k)$;
- 7 $ListId_{\hat{k}} \leftarrow [ListId_{\hat{k}}; i]$;
- 8 Update values for each μ_k
- 9 **return** $ListId_k$;

at which the camera can capture the PPG signal properly and clearly. Typical size of pinhole camera is from 0.33 to 0.58mm [46], which is too small to accurately manipulate. Since the divider is not always in the middle of the image, to precisely allocate the region for Red and NIR, a vision technique is required to subsequently split the two areas. Under the incandescent light, the two areas appeared with two different colors (red and green). The distance between two pixels p_i and p_j giving its chromatic characteristic is defined as $d(p_i, p_j) = \sqrt{\sum_{c=1}^3 (p_i(c) - p_j(c))^2}$, where $p_i(c)$ indicates the intensity of pixel i in color channel c . The detection can be formalized as a segmentation problem which can be achieved by using the K-means clustering (Algorithm 1). We initialize two pixels as the central means of each group and assign the others following the condition $\hat{k} = \operatorname{argmin}_{k=1,2} d(p, \mu_k)$. \hat{k} is the group index that the candidate pixel p is assigned to and μ_k is the central mean of group k . After all pixels are distributed into each category, we update the mean value and repeat the process until the number of iteration exist a predefined limit as described.

The PPG signal is obtained by taking the average of the intensity of the region. However, not all the pixels contribute to the signal equally, some are only noise. Therefore, to amplify the signal, a filtering procedure based on the characteristic of the PPG itself is applied. The phenomena of PPG signal is to describe the blood flow characteristic, thus, it should present some types of pulse waveform. In other words, their frequency should be bounded within the range of our heart beat. Given that information as a clue, we divide each segment into small cell and measure the frequency of each cell across the time. The sub PPG signal generated by one specific cell will be converted into the frequency domain to detect the highest peak. If the dominant frequency lays in between the lowest and highest allowable heart rate, the cell is considered to belong to the interest region. Finally, we only block the regions that only contains the pulsatile information.

PPG Extraction and absorption ratio measurement. The PPG signal is obtained from the reflected lights are highly corrupted by noise especially in the region of NIR. Therefore, the signals need to go through a set of different layers of filtering to improve the SNR without distorting the shape of that signal. In our works, we

apply the Savitzky-Golay filtering [53] which helps to reduce the noise while still maintain the pulsatile shape. The peak-to-peak measurement is used to estimate the AC component and the DC is measured by the bottom of local PPG signal (Eq. 7).

7 MODEL FOR CAMERA-BASED INTENSITY TO SPO₂ LEVEL INFERENCE

Absorption ratio estimation (R) is measured following the equation that has been proven by Beer-Lambert law as mentioned in Section 3. However, such derivation must be modified with the flashlight light source due to the impact of high saturation and large number of outliers. To overcome the problem, we propose a hybrid structure of using RANSAC [10] and the Levenberg-Marquardt (LM) [32] optimization to obtain extinction coefficients. More specifically, given a derived model and a set of observation, LM is a gradient based method which is usually used to estimate the unknown parameters/variables in the model. Our approach attempts to minimize the gap between prediction values and the ground truth by updating the parameters following the slope of gradient. To simplify the notation for the next step, we generalize the equation of approximating SpO₂ with input R (mentioned in Section 3) as following:

$$S = \frac{a_H - b_H R}{a_H - a_O + [b_O - b_H]R}, \quad (11)$$

where a_O, a_H, b_O and b_H are the extinction coefficients of two wavelengths. In this case, finding the system model is similar to identify the values of a_O, a_H, b_O and b_H given a set of input N pairs $\{s^i, R^i, i = \overline{1, N}\}$. We formulate the problem as an optimization with $\beta = [a_O, a_H, b_O, b_H]$ are the unknown variables.

$$\hat{\beta} = \underset{\beta}{\operatorname{argmin}} \sum_{i=1}^N \|s_i - S(\beta, R_i)\| \quad (12)$$

We can derive the optimal solution for these variables by iteratively updating with a portion of gradient $\beta_{t+1} = \beta_t - \gamma \mathbf{J}_t$, where $\mathbf{J}_t = \frac{\partial S(\beta_t)}{\partial \beta_t} = \begin{bmatrix} \frac{\partial S(a_O)}{\partial a_O} & \frac{\partial S(a_H)}{\partial a_H} & \frac{\partial S(b_O)}{\partial b_O} & \frac{\partial S(b_H)}{\partial b_H} \end{bmatrix}$ is the Jacobian matrix [48]. The choice of step value γ has a critical impact on the performance. In Levenberg and Marquardt model, the step variable, called γ , is a function of residuals as following $\gamma = (\mathbf{J}^T \mathbf{J} + \lambda I)^{-1} (\mathbf{J}^T r)$, where $r = \sum_{i=1}^N \|s_i - S(\beta, R_i)\|$ is the residual estimated at each iteration (T is the matrix transpose operator). The λI term makes sure that $\mathbf{J}^T \mathbf{J} + \lambda I$ is always invertible and lambda is the damping factor used to control the time of convergence. In practice, lambda can be set to equal to 1. Following this model, we optimize the extinction coefficients adopting the Lavenberg and Marquardt algorithm. In particular, we derive the Jacobian matrix by taking the partial derivative of each coefficient:

$$\mathbf{J} = \begin{bmatrix} \frac{\partial S(a_O)}{\partial a_O} & \frac{\partial S(a_H)}{\partial a_H} & \frac{\partial S(b_O)}{\partial b_O} & \frac{\partial S(b_H)}{\partial b_H} \end{bmatrix} = \begin{bmatrix} \frac{(a_H - b_H R)}{g(\beta)} & \frac{(-a_O + b_O R)}{g(\beta)} & \frac{R(b_H R - a_H)}{g(\beta)} & \frac{R(a_O - b_O R)}{g(\beta)} \end{bmatrix} \quad (13)$$

, where $g(\beta) = (a_H - a_O + (b_O - b_H)R)^2$. We summarize the process of estimating the four coefficients as in Algorithm 2.

Recall that we are using components in off-the-shelf smartphone, i.e., flash light and embedded camera sensor, this results in intensive

Algorithm 2: Extinction coefficients estimation based Levenberg – Marquardt optimization.

input : $s, R, MaxIte, \epsilon, \lambda$ - The set of ground truth SpO₂, the absorption ratio R , maximum number of iteration, minimum error and the damping factor.
output: $\hat{\beta}$ - The optimal four coefficients $\hat{\beta} = [\hat{a}_O, \hat{a}_H, \hat{b}_O, \hat{b}_H]$

- 1 Initialize values for β_0 according to the expected wavelength.
- 2 /* Finding the optimal β^* */
- 3 **for** $t = 0 \rightarrow MaxIte$ **do**
- 4 $r_t \leftarrow \sum_{i=1}^N (s_i^i - S(\beta_t, R^i))$
- 5 $\mathbf{J}_{t+1} \leftarrow \frac{\partial S(\beta_t, R)}{\partial \beta_t}$ following Equation 13
- 6 $\beta_{t+1} \leftarrow \beta_t + (\mathbf{J}^T \mathbf{J} + \lambda I)^{-1} (\mathbf{J}^T r)$
- 7 **if** $r < \epsilon$ **then**
- 8 **break**;
- 9 **return** β_t ;

Algorithm 3: RANSAC optimization based Levenberg – Marquardt model.

input : $s, R, k, MaxIte$ - The set of ground truth SpO₂, the absorption ratio R , the minimum number to be inlier set and the maximum iterations.
output: $\hat{\beta}$ - The optimal four coefficients $\hat{\beta} = [\hat{a}_O, \hat{a}_H, \hat{b}_O, \hat{b}_H]$

- 1 Initialize values for $\hat{\beta}$ /* Finding the optimal β^* */
- 2 **for** $t = 0 \rightarrow MaxIte$ **do**
- 3 /* Sampling a subset and verify possible inliers.*/
- 4 $X = \{s^q, R^q, q = \overline{1, K}\} \leftarrow \text{SubSamplingPoints}(s, R)$
- 5 $\hat{\beta}_t \leftarrow \text{Levenberg_Marquardt_Opt}(X)$ using Algorithm 2
- 6 $I_t \leftarrow \text{Validate}(\hat{\beta}_t, \{s, R\} / X)$
- 7 **if** $\|I_t\| > k$ **then**
- 8 /* We may find a good model.*/
- 9 $e_t \leftarrow \text{ValidateError}(\beta_t, s, R)$
- 10 **if** $e_t < \hat{e}$ **then**
- 11 $\hat{\beta} \leftarrow \beta_t, \hat{e} \leftarrow e_t$
- 12 **return** β_t ;

noises into our system. Thus, not all the pairs of s_i, R_i are cooperative. Some of the pairs are redundant and therefore reducing the accuracy of estimation. More importantly, as there is no prior information about the relation between s and R , blindly justifying which pairs are useful for the model is one of the directions. However, such approach cannot provide optimized solution. Instead, we indirectly measure the information that each data point contributes to the existing model. Then, we choose those pairs that have highest contribution as the inliers. Such technique is called RANdom SAMple Consensus (RANSAC). We adopt this technique for our model and present the procedure as in Algorithm 3.

To summary, a subset of data is randomly withdrawn from the whole dataset and proceeds to the Lavenberg Marquardt optimization to obtain the possible coefficients. Then, we select points that are less than 2% of error to be possible inliers. If the total number of



Figure 10: Experiment setup to compare PhO₂ with other 4 pulse oximeters

possible inliers is less than a predefined k , it is qualified to compare with existing model with the input is the whole dataset. The final output will have the smallest error among those candidates.

8 PERFORMANCE EVALUATION

In this section, we first present key results of performing the real-time SpO₂ measurement using PhO₂ system. Next, we evaluate the sensitivity of PhO₂ to extract the usable and reliable PPG signal from the images captured by the smartphone's camera. By deploying the mobile application, we further illustrate the physical efficiency of our proposed system in terms of power consumption and processing time. Finally, we analyze the surveying of users' experience of using PhO₂ system to measure their SpO₂ level.

8.1 Experimental Methodology

To evaluate the performance of the PhO₂ pulse oximetry system, we conducted our experimental studies in a normal office environment. The light source is supplied by the phone's built-in flash with noise coming from the incandescent lights in the room. The participant demographics can be found in Table 1. A board IRB was submitted for this study from the Colorado Multiple Institution Review Board.

We test our system (PhO₂) altogether with (1) a FDA-approved, official in-hospital device (Nellcor PM10N [7]), (2) a cheap fingertip pulse oximeter (FACELAKE CMS50E [6]), (3) Digidoc app [17] on iPhone 6, and (4) iCare Health Monitor app [20] on Samsung Galaxy S5.

The Nellcor PM10N is provided by Children's Hospital Colorado with the password for full access to measure and manipulate patients' data. Nellcor is one of the pioneer brands in manufacturing pulse oximeter and has been frequently used as ground truth evidence [9, 14, 31, 50]. Therefore, the device is creditable for giving baseline measurements in our experiments. On the other hands, the two mobile applications on iOS and Android only provide discrete measurement, thus the recorded data were noted down and aligned manually for the sake of comparison. This experiment is tested on six subjects with various ages, ethics and genders. Each subject

Table 1: Demographic description of participants

Participant Demographics	
Age (years)	25-32 years old
Oxygen Saturation (%)	82-97
Gender Ratio	3 male: 3 female
Ethnicity	Asian: 4, White: 2

is asked to follow a clinical instruction of breathing sequence in order to correctly reduce the blood oxygen level, in which they are asked to exhale and inhale heavily for six consecutive times and hold their breath upto their limitation. The exhale and inhale sequences help to release most of the air from the lung, thus the SpO₂ reduction process in the subjects' body can be observed easily. The whole process takes thirty minutes and is repeated five times. The oxygen level of the subject is measured simultaneously using our PhO₂ and the four devices described above (Figure 10 shows the setup of all devices on subject's fingers).

8.2 PhO₂ System Performance

In this section, we evaluate the performance of PhO₂ within 6 subjects and report the results comparing with the Nellcor PM10N. The experimental methodology is presented in the earlier Section (Sec. 8.1). Figure 11 presents the fine-grained SpO₂ predictions generated by PhO₂ for each subject. The evaluation results show that PhO₂ not only produces small error rates of SpO₂ level measurement but also illustrates the trend of oxygen level. This level of details has not been addressed with most of current smartphone-based approaches. The trend of oxygen level predicted by our system (blue line) is similar to the measurement of Nellcor device. For example, in case of the measurement for the fifth subject, the estimated results by ground truth device starts at 96% and then goes up to 99%. Meanwhile, our system reports from 94% to 98%. In the last case, the subject drops the oxygen level to below 82%, which is the same as our prediction. The interesting point is that our system responds faster than the ground truth because when the subject performs the hyperventilating and begins to hold his/her breath, the oxygen level decreases right after that; when the subject starts to inhale, the oxygen level increases. The patterns of results show that our system can predict and follow the tendency of SpO₂ level strictly even when oxygen level changes significantly.

Figure 12 summarizes the evaluation of our system with respect to all subjects (each individual and general in total). The system can measure the level of oxygen with 80th percentile error less than 3.5%. The mean and standard deviation of the absolute error rate are 2.5% and 1.62%, respectively. The mean absolute error rate is similar to that of well-known pulse oximeters, which were reported to give the prediction with 2% of mean absolute error at normal condition [62]. In addition, the standard deviation of absolute error rate achieved by PhO₂ can be reduced by averaging together many measurements over a period of time, before any decision would be made about a patient's condition. Therefore, the error rate of our system is sufficient for a home care device which does not need a very high accuracy. In some cases, physicians only concern when it is below a certain threshold. For example, the Pediatric Asthma Score [49] identifies patients are severity if their blood oxygen level is lower than 90%. In addition, to have a better view on the system performance, we conduct the test of Kendall correlation coefficients between prediction and ground truth. Figure 13 displays the result with Kendall's τ equal to 0.72 showing that the two variables are relatively matched. In details, from subject 1 to 5, the error rate is stable and close to the general case. This group of subjects includes different races, ages and genders but their demographic characteristics does not effect our system function. In fact, the factors that can defect the system from our observation is

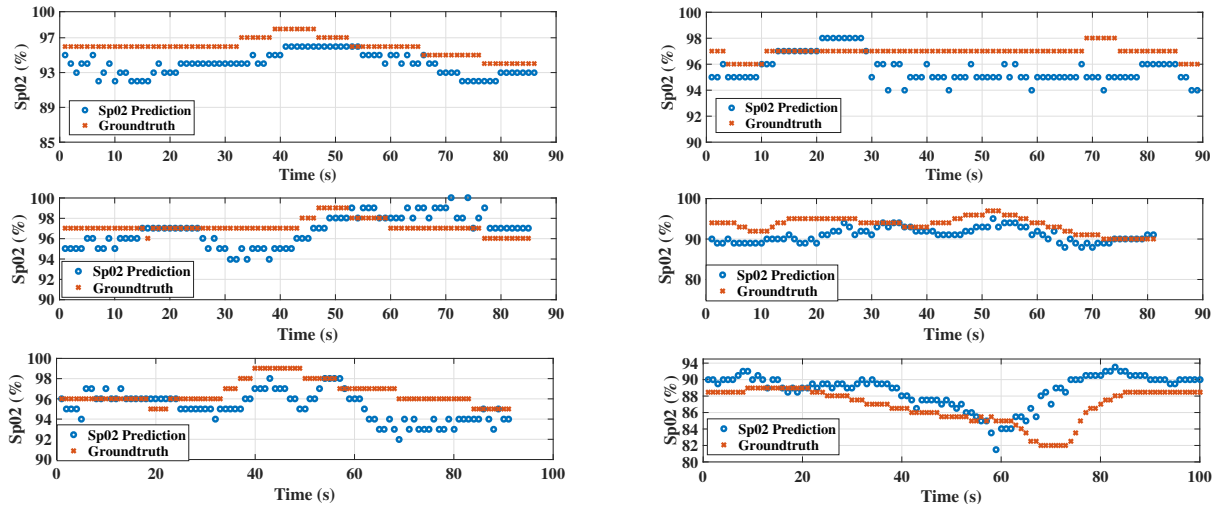


Figure 11: Fine-grained evaluation on prediction of oxygen level of 6 participants

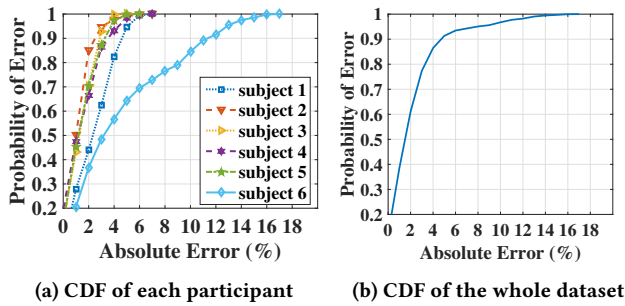


Figure 12: Distribution of error rates between PhO₂ with base-line is the Nellcor device

contact pressure and sensitivity of the system with respect to light condition. Contacting pressure is managed by pressure detection algorithm and the change of light environment is handled by the ROI detection and the design of our add-on.

The existing apps, on the other hand, represented by Digidoc (iOS) and iCare Health Monitor (Android) show their performance in Figure 14 with all subjects evaluated in our system and the groundtruth is captured by the Nellcor device. The mean absolute error of Digidoc and iCare Health Monitor are 5% and 4.36% respectively. The results clearly explain how the apps would fail to keep track on low oxygen levels. Moreover, unlike the PhO₂, they only operate as one-time measurement and thus, are unable to present continuous records.

8.3 Sensitivity Analysis

Impact of wavelength selection. Since our primary goal is to provide an evidence that combining different layers of filters can extract the desired NIR lights. This section aims at assisting our justification before is reasonable. Relying on the nature phenomena of gradient descend is all about to search for the local maxima in the set of possible solution. Obviously, initial solution is the factor that helps to define the performance of the optimization. Our intuition of conducting the experiment is to look for the relation between the optimal solution and wavelength selection. The expectation

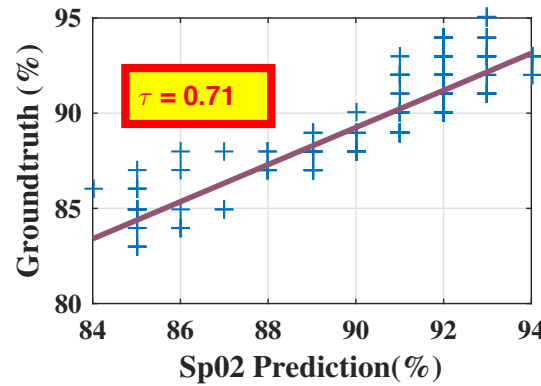
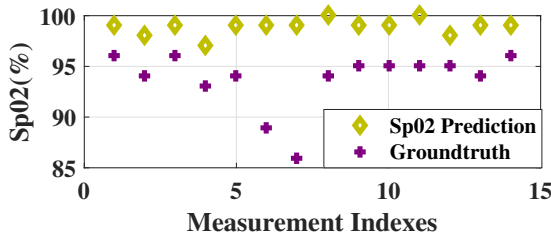


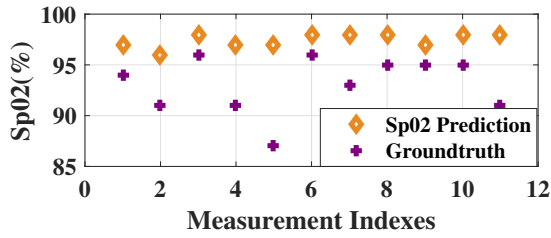
Figure 13: Kendall rank correlation coefficient between PhO₂ and base-line.

relies on the fact that only NIR wavelengths aligning with our optimization model can provide a high prediction. Starting at 610nm and going down to 602nm, the performance gradually decreases as shown in 19 which satisfies our assumption. The lights captured in that region cannot be the visible lights since those wavelength are reasonably fails to predict the oxygen level. In addition to the optimization model, the linear calibration shows its limit capability in dealing with high complex problems. Specifically, Figure 15 shows that the average accuracy linear calibration is about 94% while the one with non-linear calibration can serve up to 97%. By looking at the CDF function, the efficiency of nonlinear calibration is even more remarkable since the confident level of the linear model to achieve error rate less than 3% is only 10%.

Mitigating users' pressure issue. We collected data for pressure hardness level from twelve subjects. Each subject is asked to record multiple videos with different finger postures while using PhO₂. Each video is processed by pressure detection algorithm (described in Section 6.1) in order to classify each video frame into one of three pressure states. Figure 16 shows the calculated FFT amplitude of multiple extracting sequences from one subject, while figure 17 presents the mean and distribution of the calculated FFT amplitude from all subjects. The results of the mean values between



(a) DigiDoc (iOS)



(b) iCare Health Monitor (Android)

Figure 14: Performance evaluation of two representative applications.

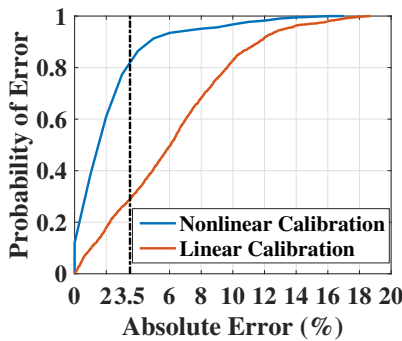


Figure 15: Comparison between linear and non linear calibration in term of system performance.

each of three states are clearly distinct. In addition, the algorithm is also tested in real-time processing as shown in Figure 18, in which test subject changes his/her pressure on fingertip continuously. While using 0.5 seconds overlapping window for detection, our algorithm misinterprets the pressure state mostly at the second of transition between two different states, especially from weak to hard pressure state and vice versa.

8.4 User Experience Survey

We asked the subjects to take a survey about their experience of using our PhO₂ prototype after their experiment period. Specifically, our questionnaire concentrates on the comfort, safety, and the usability of the device. Figure 20 shows all the questions and their results. The scale is from 1 to 5 corresponding to “Strongly Disagree” and “Strongly Agree”, respectively.

Overall, the results show the users’ agreement of being highly satisfied to use PhO₂ for the SpO₂ level measurement. The reason given is because PhO₂ is friendly to use, quick to operate, and light-weight to carry. Also, 4 in 6 subjects stated that our PhO₂ provides

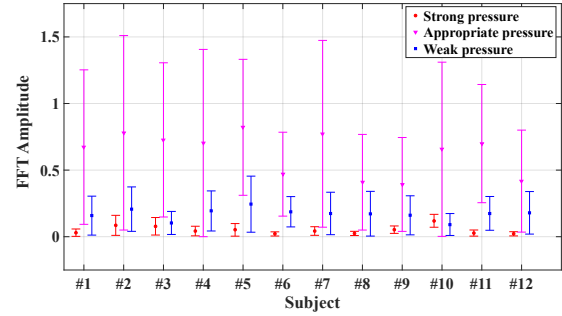


Figure 16: Hardness of the fingertip pressed on the PhO₂ add-on across subjects.

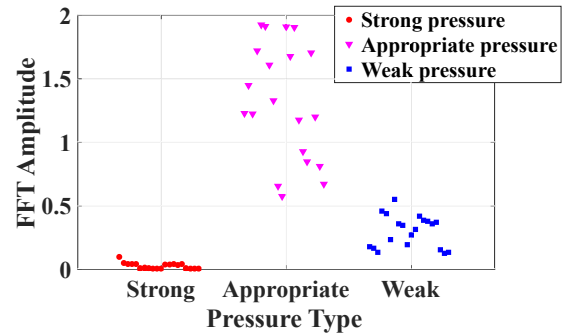


Figure 17: Hardness of the fingertip pressed on the PhO₂ add-on for 1 subject.

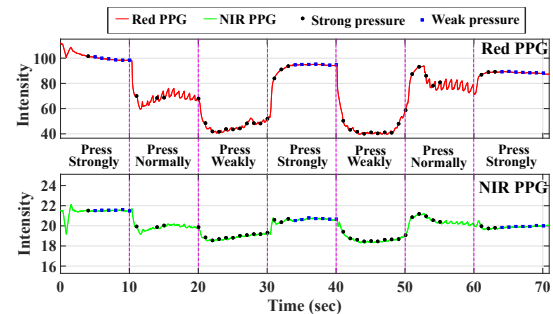


Figure 18: Real-time pressure state detection.

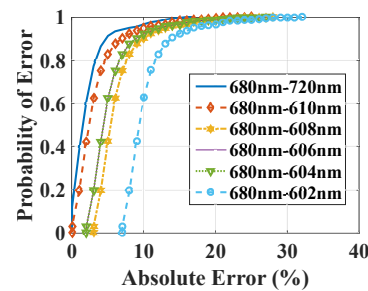


Figure 19: Results of selecting different pairs of wavelength

more comfort than the existing commercial pulse oximeters. However, some of them raised their concern about the high temperature generated from the flashlight after 10 minutes of continuously turning it on as well as placing their fingertip on it. We believe that this concern will be eliminated in real life scenarios when PhO₂ is used

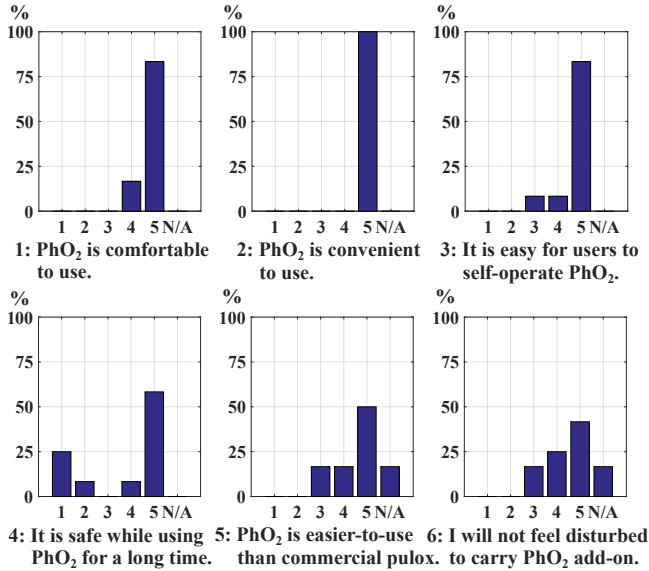


Figure 20: User Experience Questionnaire Results

in less than 5 minutes for each time of measurement. In overall, the user study showed the possibility and promise of our PhO₂ device to be adopted by users who require a management of their SpO₂.

9 DISCUSSIONS

Limitations. First limitation is the long initialization delay of the system. In the current design, PhO₂'s algorithms introduce undesirable delays for approximate the ROI, estimating pressure, and SpO₂ measurement. With our current setup, the ROI takes 6 seconds, pressure detection requires 1 seconds, and SpO₂ measurement requires 6 seconds of data. This meant that the system will not be able to output results for the first 12 seconds before it can monitor the SpO₂ level continuously. Secondly, PhO₂ has only been evaluated with in-lab environment. We obtained regional IRB for our in-clinic study that is conforming FDA procedure. An extensive study with n=10 subjects will be conducted to evaluate PhO₂ using hypoxia procedure (i.e. bringing oxygen level of a subject gradually down from normal range (95%-100%) down to extremely low range (65%-70%)) for validation. Lastly, we have only tested PhO₂ on limited number of smartphone devices. Though the device-to-device variations are considered from the design of our system, we would expect variations in the accuracy on different hardware. Future study will include a much broader ranges of devices with different diode for flashlight and camera supplier.

Potential Applications. The techniques developed in this paper have a potential to apply to other sensing domains such as substance detection using mobile phone flashlight and camera. For example, the same technique might potentially benefits anemia diagnosis and skin disease detection. The ability to collect SpO₂ might allow PhO₂ to be used for cardiopulmonary disease (e.g. heart failure and congenital heart disease have changed in oxygen level). More significantly, as monitoring SpO₂ levels is clinically standard for screening chronic respiratory diseases and assessing their severity, our PhO₂ system can be used as a light-weight solution for

chronic patients to check their SpO₂ level periodically. Additionally, by doing such the periodic SpO₂ check, our system can further predict the upcoming health problem (e.g., asthma) and quickly react against the patient's health situation, which begins getting worse. For instance, the mobile app can automatically activate a call to a medical doctor for a confirmation of his/her saturation level drops. As a result, from those who need Telehealth monitoring, our PhO₂ system can provide cost-effective strategy to support the clinical routine to follow up the patients. In addition to being mobile, smart phones are ubiquitous and this technology could potentially bring this key clinical physical finding to the global communities which are unable to purchase standard pulse ox technology due to the cost or logistic constraints (e.g. third-world countries or remote geographical areas). Finally, not only working independently, our proposed techniques can further be integrated into existing low-cost sensing systems such as the in-ear physiological sensor developed in [39] or breathing volume estimation in [67] to provide additional data sources, which is useful for improving their prediction performance.

10 CONCLUSIONS

In this paper, we presented PhO₂, a phone-based oxygen level estimation system using COTS phone's camera and flashlight. Since the smartphones' camera and flashlight are not designed for this purpose, it leads to number of challenges includes the lack of IR light from the flashlight, the lack of mathematical model to convert camera-based intensity ratio to SpO₂ level, the noisy signal captured by camera, and the unstable and undesirable pressure at users' finger contact area. We provided a carefully hardware design and a set of algorithms to overcome these challenges and making phone-based non-invasive SpO₂ level measurement possible. We also conducted a set of experiments to evaluate the performance of PhO₂. The evaluation results showed that PhO₂ obtained high performance of 3.5 % of estimation accuracy which is considered clinically sufficient by FDA standards. Lastly, we discussed the limitations of the current system, identifying its potential extension and future work; and highlighted PhO₂ potential applications.

11 ACKNOWLEDGMENTS

We thank the shepherd Neal Patwari and the anonymous ACM SenSys reviewers for their insightful comments. This research is partially supported by the Schramm Foundation, the Colorado Advanced Industries Accelerator (AIA), and U.S. National Science Foundation grant #1602428.

REFERENCES

- [1] 680nmFilter 2017. Visible Bandpass Filter —680nm FWHM 10nm. <https://goo.gl/PhLd8x>. (2017).
- [2] Geeta S. Agashe, M.B.B.S., Joseph Coakley, B.S., and Paul D. Mannheim, Ph.D. 2006. Forehead Pulse Oximetry Headband Use Helps Alleviate False Low Readings Likely Related to Venous Pulsation Artifact. *Anesthesiology* 105, 6 (2006).
- [3] BCIWW1000 2017. BCI WW1000 Spectro2 Hand Held Pulse Oximeter with Ear Clip Sensor. <https://goo.gl/xPsw1F>. (2017).
- [4] John W Berkenbosch and Joseph D Tobias. 2012. Comparison of a New Forehead Reflectance Pulse Oximeter Sensor With a Conventional Digit Sensor in Pediatric Patients. *Respiratory Care* 51, 7 (2012), 726–731.
- [5] J. Brimacombe, C. Keller, and J. Margreiter. 2000. A pilot study of left tracheal pulse oximetry. *Anesth Analg.* 91, 4 (2000), 1003–1006.
- [6] cms50e 2017. CMS-50E OLED Fingertip Pulse Oximeter. <https://goo.gl/FKP1aZ>. (2017).

- [7] covidien 2017. Nellcor™ Portable SpO₂ Patient Monitoring System, PM10N. <https://goo.gl/bxWG7R>. (2017).
- [8] Steve Cunningham and Ann McMurray. 2006. The availability and use of oxygen saturation monitoring in primary care in order to assess asthma severity. *Primary Care Respiratory Journal* 15 (2006), 98 – 101.
- [9] Marco Fernandez, Kathy Burns, Beverly Calhoun, Saramma George, Beverly Martin, and Chris Weaver. 2007. Evaluation of a New Pulse Oximeter Sensor. *American Journal of Critical Care* 16, 2 (2007), 146–152.
- [10] Robert B Fisher. 2002. The RANSAC (random sample consensus) algorithm. (2002).
- [11] Sotirios Fouzas, Kostas N. Pfriftis, and Michael B. Anthracopoulos. 2011. Pulse Oximetry in Pediatric Practice. *Pediatrics* 128, 4 (2011), 740–752.
- [12] Matthew J. Hayes and Peter R. Smith. 1998. Artifact reduction in photoplethysmography. *Applied Optics* 37, 31 (Nov 1998), 7437–7446.
- [13] Jeffrey M Haynes. 2007. The ear as an alternative site for a pulse oximeter finger clip sensor. *Respiratory care* 52, 6 (2007), 727–729.
- [14] Jeffrey M Haynes. 2012. The Ear as an Alternative Site for a Pulse Oximeter Finger Clip Sensor. *Respiratory Care* 52, 6 (2012), 727–729.
- [15] Heart Rate Pulse Oximeter 2017. Heart Rate Pulse Oximeter. <https://goo.gl/nZWuqU>. (2017).
- [16] History 2017. History of pulse oximeter. <https://goo.gl/5N0GDR>. (2017).
- [17] Kelly Hodgkins. 2014. Daily App: digiDoc Pulse Oximeter tries to measure your heart rate and oxygen levels. *Modern Healthcare* (2014).
- [18] Homedics 2017. Homedics Px-100 Deluxe Pulse Oximeter. <https://goo.gl/qaomPz>. (2017).
- [19] Cheng-Yang Huang, Ming-Che Chan, Chien-Yue Chen, and Bor-Shyh Lin. 2014. Novel Wearable and Wireless Ring-Type Pulse Oximeter with Multi-Detectors. *Sensors* 14, 9 (2014), 17586–17599.
- [20] iCareOxygenMonitor 2017. iCare Oxygen Monitor. <https://goo.gl/B5hyjW>. (2017).
- [21] Instant Pulse Oximeter 2017. Instant Pulse Oximeter. <https://goo.gl/0059Qx>. (2017).
- [22] Instant Pulse Rate 2017. Instant Pulse Rate. <https://goo.gl/B3FnkT>. (2017).
- [23] Invasive Blood Test 2017. Invasive Tests and Procedures. <https://goo.gl/sKxCYB>. (2017).
- [24] iPhone6 Camera Lens 2017. iPhone6 Camera Lens. <https://goo.gl/ppB0xZ>. (2017).
- [25] Priya Jegatheesan, Dongli Song, Cathy Angell, Kamakshi Devarajan, and Balaji Govindaswami. 2013. Oxygen Saturation Nomogram in Newborns Screened for Critical Congenital Heart Disease. *Pediatrics* 131, 6 (2013), e1803–e1810.
- [26] Christina Jrgensen and Toke Bek. 2014. Increasing Oxygen Saturation in Larger Retinal Vessels After Photocoagulation for Diabetic Retinopathy Oxygen Saturation in Diabetic Retinopathy. *Investigative Ophthalmology & Visual Science* 55, 8 (2014), 5365.
- [27] W. Karlen, J. Lim, J. M. Ansermino, G. Dumont, and C. Scheffer. 2012. Design challenges for camera oximetry on a mobile phone. *2012 Annual International Conference of the IEEE Engineering in Medicine and Biology Society* (2012).
- [28] J G Kim and H Liu. 2007. Variation of haemoglobin extinction coefficients can cause errors in the determination of haemoglobin concentration measured by near-infrared spectroscopy. *Physics in Medicine and Biology* 52, 20 (2007), 6295.
- [29] F. Lamonaca, D. L. Carn, D. Grimaldi, A. Nastro, M. Riccio, and V. Spagnolo. 2015. Blood oxygen saturation measurement by smartphone camera. In *Medical Measurements and Applications (MeMeA), 2015 IEEE International Symposium on*. IEEE, 2015.
- [30] leeFilter 2017. LEE Filters 738 JAS GREEN. <https://goo.gl/zLodlp>. (2017).
- [31] Michael S Lipnick, John R Feiner, Paul Au, Michael Bernstein, and Philip E Bickler. 2016. The Accuracy of 6 Inexpensive Pulse Oximeters Not Cleared by the Food and Drug Administration: The Possible Global Public Health Implications. *Anesthesia & Analgesia* 123, 2 (2016), 338–345.
- [32] Manolis IA Lourakis. 2005. A brief description of the Levenberg-Marquardt algorithm implemented by levmar. (2005).
- [33] Suzanne Low, Yuta Sugiura, Dixon Lo, and Masahiko Inami. 2014. Pressure Detection on Mobile Phone by Camera and Flash. In *Proceedings of the 5th Augmented Human International Conference (AH '14)*. 11:1–11:4.
- [34] Nitzan M, Romem A, and Koppel R. 2014. Pulse oximetry: fundamentals and technology update. *Medical Devices: Evidence and Research* 7 (2014), 231–239.
- [35] Emin Maltepe and Ola Didrik Saugstad. 2009. Oxygen in Health and Disease: Regulation of Oxygen Homeostasis—Clinical Implications. *Nature Reviews Molecular Cell Biology* 65 (2009), 261–268.
- [36] Simon MC and Keith B. 2008. The role of oxygen availability in embryonic development and stem cell function. *Nature Reviews Molecular Cell Biology* 9 (2008), 285–296.
- [37] Sanjay V. Mehta, Patricia C. Parkin, Derek Stephens, and Suzanne Schuh. 2004. Oxygen saturation as a predictor of prolonged, frequent bronchodilator therapy in children with acute asthma. *The Journal of Pediatrics* 145, 5 (2004), 641 – 645.
- [38] Payal Modi, Richard B. Mark Munyaneza, Elizabeth Goldberg, Garry Choy, Randheer Shailam, Pallavi Sagar, Sjurk J. Westra, Solange Nyakubaya, Mathias Gakwerere, Vanessa Wolfman, Alexandra Vinograd, Molly Moore, and Adam C. Levine. 2013. Oxygen Saturation Can Predict Pediatric Pneumonia in a Resource-Limited Setting. *The Journal of Emergency Medicine* 45, 5 (2013), 752 – 760.
- [39] Anh Nguyen, Raghda Alqurashi, Zohreh Raghebi, Farnoush Banaei-kashani, Ann C. Halbower, and Tam Vu. 2016. A Lightweight and Inexpensive In-ear Sensing System For Automatic Whole-night Sleep Stage Monitoring. In *Proceedings of the 14th ACM Conference on Embedded Network Sensor Systems CD-ROM*. ACM, 230–244.
- [40] NIR filter 2017. NIR filter thinkness. <https://goo.gl/lkPedL>. (2017).
- [41] nonin 2017. NONIN 8000Q2 Ear Clip Sensor. <https://goo.gl/P2a9W1>. (2017).
- [42] Optical Spectrum Analyzer 2017. Ando Model AQ6315E Optical Spectrum Analyzer. <https://goo.gl/apKy2C>. (2017).
- [43] oxiMax 2017. Nellcor OxiMax D-YSE Ear Clip Sensor. <https://goo.gl/Wajkva>. (2017).
- [44] Christian L Petersen, Tso P Chen, J Mark Ansermino, and Guy A Dumont. 2013. Design and evaluation of a low-cost smartphone pulse oximeter. *Sensors* 13, 12 (2013), 16882–16893.
- [45] C. L. Petersen, H. Gan, M. J. MacInnis, G. A. Dumont, and J. M. Ansermino. 2013. Ultra-low-cost clinical pulse oximetry. In *2013 35th Annual International Conference of the IEEE Engineering in Medicine and Biology Society (EMBC)*. IEEE, 2013.
- [46] Pin hole size 2017. Camera pinhole size. <https://goo.gl/S0Bi4c>. (2017).
- [47] quest 2017. Quest Q1911 Oximeter. <https://goo.gl/24LWjh>. (2017).
- [48] Dr Osbaldo Resendis-Antonio. 2013. Jacobian Matrix. In *Encyclopedia of Systems Biology*. 1061–1062.
- [49] Safety and Quality Collaborative Asthma Management Pathway (ED and IP) 2017. Childrenfhis Hospital Association of Texas Safety and Quality Collaborative Asthma Management Pathway (ED and IP) . <https://goo.gl/vN676X>. (2017).
- [50] Lynn Schallom, Carrie Sona, Maryellen McSweeney, and John Mazuski. 2007. Comparison of forehead and digit oximetry in surgical/trauma patients at risk for decreased peripheral perfusion. *Heart & Lung: The Journal of Acute and Critical Care* 36, 3 (2007), 188–194.
- [51] ScottPrahL 2017. Scott PrahL. Tabulated molar extinction coefficient for hemoglobin in water. 1998. <https://goo.gl/7SBwzQ>. (2017).
- [52] C. G. Scully, J. Lee, J. Meyer, A. M. Gorbach, D. Granquist-Fraser, Y. Mendelson, and K. H. Chon. 2012. Physiological Parameter Monitoring from Optical Recordings With a Mobile Phone. *IEEE Transactions on Biomedical Engineering*, 303–306.
- [53] Mary C Seiler and Fritz A Seiler. 1989. Numerical recipes in C: the art of scientific computing. *Risk Analysis* 9, 3 (1989), 415–416.
- [54] sm 2017. SM-165. <https://goo.gl/5N0GDR>. (2017).
- [55] Kendric C Smith. 1991. The photobiological basis of low level laser radiation therapy. *Laser Therapy* 3, 1 (1991), 19–24.
- [56] SolidWorks 2017. SOLIDWORKS. <http://www.solidworks.com/>. (2017).
- [57] Norbert Stubn and Niwayama Masatsugu. 2008. Non-invasive calibration method for pulse oximeters. *Periodica Polytechnica Electrical Engineering* (2008), 91–94. DOI: <https://doi.org/10.3311/pp.ee.2008-1-2.11>
- [58] Sarah Sykes, Ruth Kingshott, and Robert Primhak. 2011. Awake and asleep oxygen saturations in infants with chronic neonatal lung disease. *Acta Paediatrica* 100, 8 (2011), 1087–1091.
- [59] These Medical Apps Have Doctors and the FDA Worried 2017. These Medical Apps Have Doctors and the FDA Worried. <https://goo.gl/rEXYGD>. (2017).
- [60] Vigor Sp02 2017. Vigor Sp02. <https://goo.gl/MFfsTJ>. (2017).
- [61] Edward Jay Wang, William Li, Doug Hawkins, Terry Gernsheimer, Colette Norby-Slycord, and Shwetak N. Patel. 2016. HemaApp: Noninvasive Blood Screening of Hemoglobin Using Smartphone Cameras. In *Proceedings of the 2016 ACM International Joint Conference on Pervasive and Ubiquitous Computing (UbiComp '16)*. 3320–3338.
- [62] Ralston AC Webb RK and Runciman WB. 1991. Potential errors in pulse oximetry. II. Effects of changes in saturation and signal quality. *Anaesthesia* 46, 3 (1991), 207–212.
- [63] S. Wendelken, S. McGrath, G. Blike, and M. Akay. 2004. The feasibility of using a forehead reflectance pulse oximeter for automated remote triage. In *IEEE 30th Annual Northeast Bioengineering Conference, 2004. Proceedings of the*. 180–181.
- [64] J. Xiong, L. Cai, D. Jiang, H. Song, and X. He. 2016. Spectral Matrix Decomposition-Based Motion Artifacts Removal in Multi-Channel PPG Sensor Signals. *IEEE Access* 4 (2016), 3076–3086.
- [65] Y. S. Yan and Y. T. Zhang. 2008. An Efficient Motion-Resistant Method for Wearable Pulse Oximeter. *IEEE Transactions on Information Technology in Biomedicine* 12, 3 (2008), 399–405.
- [66] Jianchu Yao and S. Warren. 2004. A novel algorithm to separate motion artifacts from photoplethysmographic signals obtained with a reflectance pulse oximeter. In *The 26th Annual International Conference of the IEEE Engineering in Medicine and Biology Society*, Vol. 1. 2153–2156.
- [67] P. Nguyen, X. Zhang, A. Halbower, and T. Vu. 2016. Continuous and fine-grained breathing volume monitoring from afar using wireless signals. In *IEEE INFOCOM 2016 - The 35th Annual IEEE International Conference on Computer Communications*. 1–9.
- [68] WG Zijlstra, A Buursma, and WP Meeuwssen-van der Roest. 1991. Absorption spectra of human fetal and adult oxyhemoglobin, de-oxyhemoglobin, carboxyhemoglobin, and methemoglobin. *Clin Chem* 37, 9 (1991), 1633–1638.